Available online at www.sciencedirect.com

ScienceDirect

Procedia Earth and Planetary Science 9 (2014) 91 – 100

Procedia
Earth and Planetary Science

The Third Italian Workshop on Landslides

New advances and challenges for numerical modeling of landslides of the flow type

Sabatino Cuomo[a]*

[a]*University of Salerno, Via Giovanni Paolo II 132, Fisciano (SA) 84084, , Italy*

Abstract

Landslides of the flow types represent a worldwide natural hazard whose consequences have been largely increasing in the last decades, despite the huge efforts of the International Organizations and Scientific Communities which can provide either highly interdisciplinary approaches or enhanced sector-based studies. The former must include expertise from geology, geotechnical engineering, social sciences and economics if landslide risk reduction is pursued as final goal while the latter include detailed geotechnical analyses to simulate the multiple stages characterizing the landslides of the flow-type. Within this framework, numerical modeling has been playing an increasing role for engineering-based decisions. The present paper outlines some difficult topics recently solved or firstly tacked through advanced numerical modeling. For the failure stage, distinct modeling alternatives are applied to a relevant case study. For the post-failure stage, an enhanced numerical approach is provided to understand and forecast the transition from a slide to a flow. Furthermore, a novel numerical approach is applied for evaluating the propagation heights and velocities. Finally, open issues are outlined and possible future research developments are indicated.

Selection and peer-review under responsibility of Dipartimento di Ingegneria Civile, Design, Edilizia e Ambiente, Seconda Università di Napoli.

Keywords: triggering; post-failure; propagation; FEM; SPH.

1. Introduction

Landslides of the flow-type[1] include a wide class of phenomena still difficult to classify[2] because they involve mixtures of water, air and solid grains with percentages extremely variable in space and time. In particular, debris

* Corresponding author. Tel.: +39(0)89-964231; fax: +39(0)89-968732.
E-mail address: scuomo@unisa.it

Selection and peer-review under responsibility of Dipartimento di Ingegneria Civile, Design, Edilizia e Ambiente, Seconda Università di Napoli.
doi:10.1016/j.proeps.2014.06.004

flows[3,4] propagate in "V" shaped channels with some peculiarities: i) at the entry of channel, height and velocity of propagating mass increase, ii) along the channel, material can be entrained and large amount of water is available which cause the propagating mass to fluidize, even without liquefaction has occurred in landslide source areas, iii) at the exit of the channel, the mass may stop or continue propagating along one or more directions not known a priori, even travelling different run-out distances along each path, iv) at piedmont, mass deposition finally occurs.

Landslides of the flow-type have been deserved much attention by researchers in the last decades, due to their destructiveness and mechanical peculiarities especially related to shallow steep deposits of unsaturated collapsible coarse-grained soils. However, the analysis and forecasting of these phenomena is currently based on decomposing the whole process in multiple stages to be analyzed each with specific approaches. In particular, three main stages[4] can be distinguished: failure, post-failure and propagation.

Failure[5] stage is characterized by the formation of a continuous shear surface[6] through the entire soil mass (i.e. localized failure); alternatively, plastic strains may affect a large amount of soil originating a diffuse failure[7,8]. Failure eventually involve similar slopes in very large areas, like occurred in Southern Italy (Pizzo d'Alvano carbonate massif[9,10]), where 240 mm rainfall in 48 hours[9,11,12] triggered more than 100 shallow landslides on 4th - 5th May 1998. For this case history, the analysis of post-event data concerning the location of landslides source areas, geomorphology/hydrogeology of the massif, anthropogenic factors and source areas characteristics, point out six typical triggering mechanisms[13,14,10]. The most frequent mechanism (named M1, corresponding to 28% of 133 landslide source areas) occurred inside colluvial hollows, i.e. the so-called Zero Order Basins, which are characterized by convergent groundwater circulation inside the shallow soil deposits and temporary springs from the bedrock. Similar evidences of landsliding over large areas come from Colorado, U.S.[15].

Post-failure[16] stage is represented by a rapid generation of large plastic strains and consequent sudden acceleration of the failed soil mass; it is often accompanied with a reduction of pore water pressures, which leads to a drastic increase of the landslide mobility. Some evidences are available for the case history above mentioned; in fact, just after the event, upslope and beside the landslides source areas, more than 500 fractures were recognized on the ground surface (Fig. 1a); this clearly points out the occurrence of local slope instabilities not evolved into landslides of the flow-type because only suffering moderate displacements. Well established experimental evidences from laboratory centrifuge tests are available as well, like those performed by Take et al.[17] who show that slopes of both loose (Fig. 2a) and dense (Fig. 2b) sands can suffer landslides of the flow type, due to soil cover layering, soils permeability contrast and related transient local pore water pressures.

Propagation[4] stage includes the movement of failed soil mass from the source areas up to some kilometers far, where material stops; it entails run-out distance is one or two orders of magnitude greater than the landslide source area dimensions. Figure 1 shows that tens of shallow landslides turned into landslides of the flow-type (Fig. 1b) and traveled more than 2 km[18,19]. As a consequence, 159 victims and relevant damage to property were recorded in the four towns located at the toe of the massif. During the propagation stage, landslide volume increased due to: i) soil erosion in the gullies below and ii) incorporation of minor slides mobilized along the flanks of the gullies. Globally, bed entrainment phenomena amplified the triggered volumes by a factor of 1.5 for the largest landslides[18].

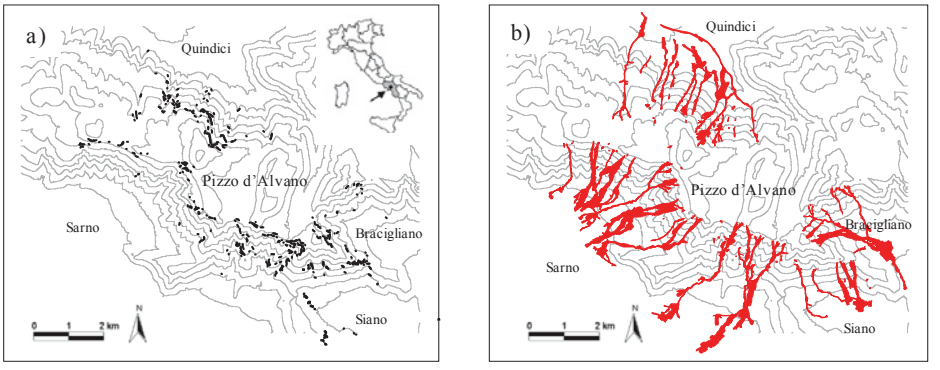

Fig. 1. Fractures recognized on the ground surface just after the 4-5th May 1998 rainstorm (a) and the occurred landslides of the flow-type (b).

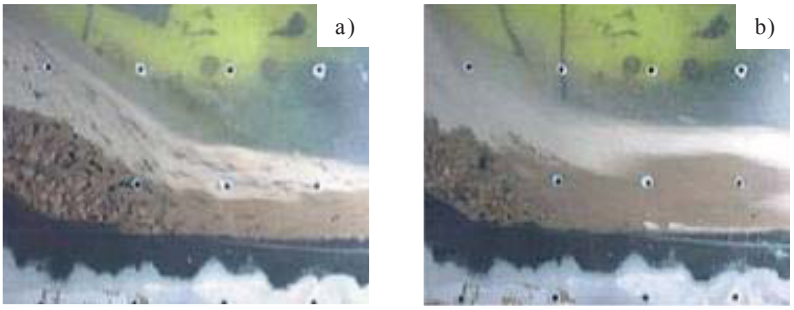

Fig. 2. Experimental evidence of flow like landslides in centrifuge slope model[17]: a) loose, b) dense soils.

The aim of the paper is to provide a novel contribution towards a unified modeling of the three stages of flow-type landslides since limited attempts have been proposed in the literature. Particularly, potentialities and limitations of advanced numerical tools are discussed within the mathematical framework proposed by Zienkiewicz et al.[20,21] for mixtures of solid grains, water and air subjected to small/large deformations. To do so, numerical models are applied to either a relevant case history of Southern Italy, for which a detailed data-set is available, or well established experimental evidences. A comprehensive discussion of achievable results is also provided and new ideas for research are elaborated within a unitary framework.

2. Methods and inputs for modeling

2.1. GeHoMadrid hydro-mechanical coupled FEM model

The adopted hydro-mechanical coupled model derives from the contributions of Zienkiewicz et al.[20,21] and Pastor et al.[22] that consider a solid skeleton and two fluid phases, water and air, which fills the voids. The skeleton is made of particles of density ρ_s with porosity n (volume percent of voids in the mixture) and void ratio e (volume of voids per unit volume of solid fraction). Movement of the fluid is considered as composed of two parts, the movement of soil skeleton and motion of the pore water relative to it. The total stress tensor acting on the mixture can be decomposed as the sum of an effective stress tensor σ' acting on soil skeleton and a hydrostatic pore pressure term p_w which for unsaturated soils with zero air pressure corresponds to the averaged pore pressure. For soil unsaturated conditions Bishop's stresses are accounted for. The governing equations[4] of the model consist in: i) balance of momentum equation for the mixture, ii) balance of mass of pore water, iii) mass conservation for pore fluid, iv) balance of momentum of pore fluid, v) a kinematic relation linking velocities to rate of deformation tensor and vi) a suitable constitutive model. Unknowns are displacements of solid skeleton and pore water pressure.

Among the constitutive models available for incrementally non-linear and non-associative geomaterials, such as coarse-grained soils, Classical Plasticity Theory is an efficient tool to combine computational simplicity and availability of data coming from standard laboratory geotechnical tests. This class of models includes the elastic perfectly-plastic Drucker-Prager and Mohr-Coloumb models, whose limited number of parameters (cohesion, friction angle, dilation angle) has motivated their wide use for practice and research.

A valuable alternative derives from Generalized Plasticity Theory[23] to which the Pastor-Zienkiewicz (PZ) model belongs. The latter is suitable to accurately describe the behavior of either loose or dense granular soils, both in drained and undrained conditions, along complex stress paths. In the PZ model, plastic deformations may occur upon either loading or unloading and they are derived without the need to define the: i) yielding surface, ii) plastic potential surface, iii) consistency law. In details, the model is completely defined once the following quantities are fixed: i) three directions (load direction n_{gL}, unload direction n_{gU} and neutral load direction n), ii) two scalars (plastic moduli H_L and H_U) and iii) the elastic tensor De. Globally, 12 parameters are defined (K_{ev0}, G_0, M_g, M_f, H_0, H_{u0}, α_g, α_f, β_1, β_0, γ, γ_u); K_{ev0} and G_0 are, respectively, the bulk modulus and shear modulus, M_g and M_f represent in the q-p' space the slope of critical state line and the slope of instability line[16], H_0 and H_{u0} are hardening modulus in loading and unloading. Calibration of these parameters can be performed through standard triaxial tests according to the

procedures indicated by Zienkiewicz et al.[21] who also provide the values of some constants incorporated in the model, named α_g, α_f, β_1, $\beta 0$, γ and γ_u. It is worth noting that M_f is univocally related to the soil relative density as suggested by Pastor et al.[23].

The governing equations of the hydro-mechanical coupled model are implemented in the "GeHoMadrid_FEM" code[22], which is used to analyze failure and post-failure stage of some landslides. It is worth noting that Cascini et al.[4] demonstrate that either standard limit equilibrium formulations or stress-strain approach with uncoupled computation for pore water pressures can be derived as special cases of the GeHoMadrid mathematical framework.

2.2. GeoFlow_SPH hydro-mechanical coupled depth-integrated SPH model

The "GeoFlow_SPH" model[24] is based on the theoretical framework of Hutchinson[25] and Pastor et al.[26] and schematizes the propagating mass as a mixture of a solid skeleton saturated with water; the unknowns are the velocity of the solid skeleton (v) and the pore water pressure (p_w).

The governing equations are: i) balance of mass of the mixture combined with the balance of linear momentum of the pore fluid, ii) balance of linear momentum of the mixture, iii) rheological equation relating soil stress tensor to deformation rate tensor and iv) kinematical relations between deformation rate tensor and velocity field.

From here, a propagation-consolidation model[24] is derived assuming that: i) pore water pressure dissipation takes place along the normal to the ground surface and ii) velocity of solid skeleton and pressure fields can be split into two components, i.e., propagation and consolidation. Since many flow-like landslides have small average depths in comparison with their length or width, the above equations can be integrated along the vertical axis and the resulting 2D depth-integrated model presents an excellent combination of accuracy and time cost.

The GeoFlow_SPH model also accounts for bed entrainment along the landslide path and the elevation of ground surface consistently decreases in time. Different empirical erosion laws[27,28] are implemented so far. The simple yet effective law proposed by Hungr[27] is used, mainly to achieve results comparable with literature. It is worth noting that: i) landslide grow rate (E_r)[27] is related to the initial and final landslide volume as well as to the travelled distance (L), ii) a nil value is assumed for velocity and pore water pressure for material entrained.

In the GeoFlow_SPH model, the Smoothed Particle Hydrodynamics (SPH) method is used which discretizes the propagating mass through a set of moving "particles" or "nodes". Information, i.e. unknowns and their derivatives, is linked to the particles and the SPH discretization consists on a set of ordinary differential equations[24]. The accuracy of the numerical solution and the level of approximation for engineering purposes depend on how the nodes are spaced and how the Digital Terrain Model (DTM) is detailed, as recently reviewed in the literature[29,30].

3. Numerical modeling and new challenges

3.1. Failure stage

The geometry of a shallow soil deposit is well schematized by the infinite slope scheme (Fig. 3) which is used to address the modeling of the failure stage through either standard or enhanced computational tools.

Pore water pressures are firstly computed integrating the Richard's equation through the FEM code SEEP/W[31]. The FEM mesh consists in 3,500 quadrilateral elements smaller than 0.4 m each. Then, slope stability conditions are evaluated through Limit Equilibrium Methods (LEM) proposed by Janbu[32] and Morgenstern and Price[33] using the commercial SLOPE/W code[31] and referring to the pore pressures computed. A rigid-perfectly plastic constitutive model is considered with the failure criterion proposed by Fredlund et al.[34] who extended the Drucker-Prager criterion to unsaturated soils. The numerical model reads: i) slope angle is 35°, soil depth is 4.5m, saturated unit weight equal to 13.1 kN/m^3, ii) Young modulus is 3,000 kPa, Poisson ratio is 0.29, iii) friction angle is 39°, cohesion is 2.5 kPa, rate of increase in shear strength due to suction[34] is 20°, nil dilation angle, iv) saturated soil conductivity equal to 10^{-5} m/s and initial soil suction equal to 5kPa, v) at the ground surface, a inflow boundary condition is assumed equal to hourly rainfall intensity from 4th to 5th May 1998, vi) evapo-transpiration neglected, vii) impervious bedrock contact expect for a spring zone with a 1.67×10^{-5} m^3/s water flux.

Seepage analysis indicates that both rainfall infiltration from ground surface and localized pore water pressures induced by spring from bedrock are responsible for slide occurrence (Fig. 3). A clear correlation is pointed out

between the time trend of the maximum pore water pressure (at point P) along the critical slip surface (Fig. 3) and the associated factor of safety (FS). It is worth noting that simulated time failure well fits the in-situ eyewitnesses[9].

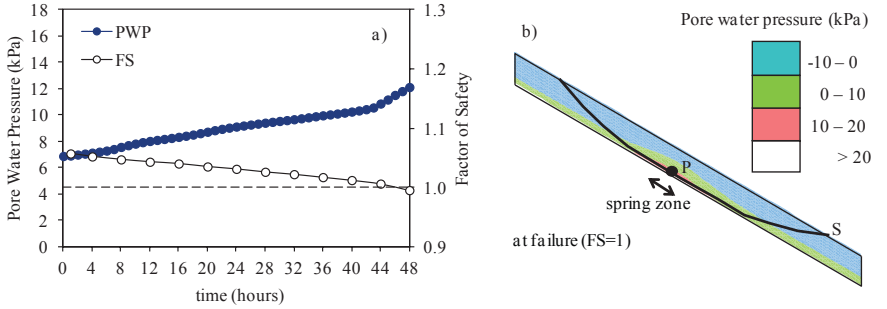

Fig. 3. (a) Time evolution of pore water pressure (PWP) at point P and factor of safety (FS) on slip surface S and (b) contour of PWP at failure.

A priori selection of the shape and depth of slip surface is a strong limitation of LEM, which does not exist in uncoupled stress-strain FEM analysis. Thus, the formation of soil cover of figure 3 is simulated by a multi-steps increase of soil depth and then transient pore water pressures are used as input for soil deformation computation. In this case it is found that high stress ratios (q/p'), shear deformations and displacements are simulated at the spring zone, due to the reduction of effective mean stress at nearly constant deviatoric stress. In particular: soil yielding causes deformations upslope due to the increase of deviatoric stress at nearly constant effective mean stress; time failure agrees in-situ eyewitnesses; simulated displacements and the amount of failing mass well match those found via LEM; simulated displacements depend on Young modulus while dilation angle plays a negligible role.

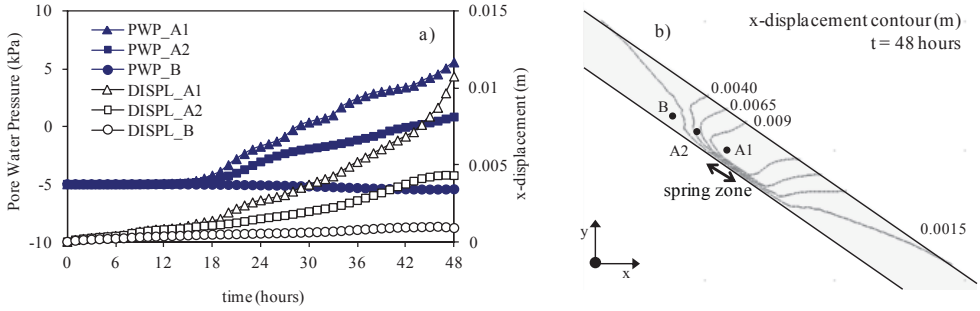

Fig. 4. (a) Time evolution of pore water pressure (PWP) and (b) x-displacement (DISPL) contour at failure.

It is worth noting that pore water pressures strongly depend on hydraulic boundary conditions (rainfall and spring from bedrock) as simulated above but soil compressibility behavior, stress and strain fields may affect pore water pressures as well. This issue requires the use of hydro-mechanical coupled approaches such as GeHoMadrid, which is tested for the previous infinite slope scheme (Fig. 3-4) using the same soil properties and boundary conditions.

The achieved results (Fig. 5) show that: i) significant plastic strains arise only for the combination of rainfall and spring from bedrock, ii) simulated slope instability scenario and the time failure well agree those obtained with previous simplified analyses (LEM and uncoupled FEM), thus highlighting their potential for capturing the global behavior of the slope. However, it is found that dilation angle plays an important role. Simulated displacements are negligible and failure not captured for a dilation angle equal to friction angle (i.e. associated flow rule). On the contrary, high pore water pressures and displacements as well as a fast build up of both variables are simulated for a nil dilation angle (i.e. not associated flow rule). This slope behavior is not captured by simplified approaches.

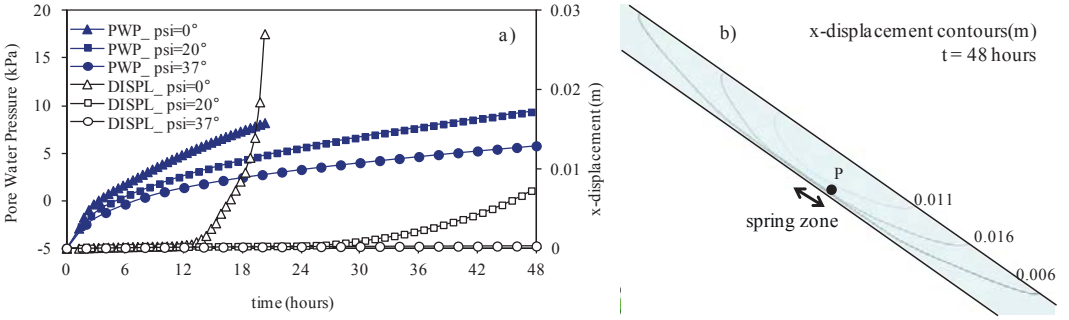

Fig. 5. (a) Time evolution of pore water pressure (PWP) and (b) x-displacement (DISPL) contour at failure depending on dilation angle.

While providing a sound framework for the analysis of failure stage, the achieved results and the available tools claim for new challenges to be addressed. For instance, hydro-mechanical coupled FEM approaches have found rare applications to detailed stratigraphies of steep shallow soil covers. This lack is motivated by: i) computational costs of FEM-based codes whether applied to slope geometry 1 - 5 m thick and 100 - 200 m long, ii) uncertainties related to slope formation process whose simulation greatly affects stress and strain fields, iii) need of efficient numerical algorithms to tackle the mechanical response of frictional (almost cohesionless) soils over steep slopes.

New advancements may also come from the validation of numerical results with monitoring data of soil stresses, pore pressures and displacements (up to failure). In fact, while it is understandable that centrifuge tests currently provide a good approximation of real slope behavior as it concerns the order of magnitude of both stresses and forces, literature reports only few examples of real slopes well monitored up to failure onset.

3.2. Post-failure stage

In the previous analyses, the possibility to distinguish between slide and flowslide[5] is prevented by the use of a simplified constitutive model, such as Druger-Prager, which is not suitable to properly simulate the mutual interaction between solid skeleton and pore water. Thus, the centrifuge tests performed by Take et al.[17] are simulated through the GeHoMadrid code, referring to the PZ constitutive model (see sect. 2.1).

Slope geometry consists in a shallow deposit 33° inclined over impervious bedrock (Fig. 6). Due to centrifuge acceleration, the equivalent prototype slope is about 15 m long and 2 m thick. Stratigraphy includes a coarser lower soil layer more permeable than upper soils. A water spring is located at the bedrock contact on the upper right corner of the slope. Experimental observations include: i) transient groundwater seepage in both layers and at the toe of the slope model, due to slope geometry and soil permeability contrast, ii) slope failure occurrence accompanied by a sudden acceleration of the failed mass in both cases of loose and dense soils, iii) decrease of pore water pressures due to slope geometry modifications after the failure onset.

The hydro-mechanical coupled FEM analysis is performed for an unstructured mesh of triangles long 0.4 m as maximum. Pore water pressure is allowed to change in space and time, starting from -5kPa throughout the slope model. The raising of water table in the upper soil layer is simulated assuming a nil pore water pressure at point E, corresponding to the water table level observed at failure during the tests. Fully saturated conditions are considered for PZ constitutive model. Soil mechanical properties[17] are given in figure 6; particularly, k_{sat}, E and H_0 were indirectly estimated/calibrated comparing the experimental evidences and the numerical results). It is worth noting that M_f derives from different relative soil density. Aimed to emphasize the role of soil relative density as an important factor for slope behavior upon failure and beyond, a limit case is assumed, which entails the equality of: critical friction angle (M_g), bulk modulus (K_{ev0}) and hydraulic conductivity for both loose and dense soils.

Simulated plastic strains significantly differ for loose and dense soil (Fig. 7) and the extent of the zone affected is larger for loose soil. In the latter case plastic strains firstly occur at the slope toe later involving a larger soil volume according to a diffuse failure style. For dense soil, plastic strains start as well from the toe of the slope but then accumulate along a specific slip surface, i.e. a “localized” failure occurs. Those differences depend on a different

value of soil relative density, as the other mechanical properties are equal in both cases. In addition, for loose soil, the simulated failure stage is faster due to higher excess pore water pressures rapidly accumulating in the slope until failure occurs. Conversely, for dense soil, either pre-failure stage entailing elastic strains or failure stage are longer in time, as measured in the experiments (Fig. 7). Independently on soil relative density, the failed mass accelerates and pore water pressure decreases in agreement with experiments[17]; in addition, the onset of a yielding zone in the upper right corner is simulated, as observed in similar centrifuge tests[35].

Despite the value of the previous results, it is still problematic to ensure that a small-strain formulation like that of "GeHoMadrid_FEM" is well suited to simulate the post-failure stage. The latter may include large displacements within the failed mass and procedures for slope geometry updating (eventually with domain remeshing) should be adopted in that case. More in general, the transition from solid to fluid is a new challenge for the analysis of post-failure stage; pioneristic attempts in that direction were recently proposed[36] but further advancement is required.

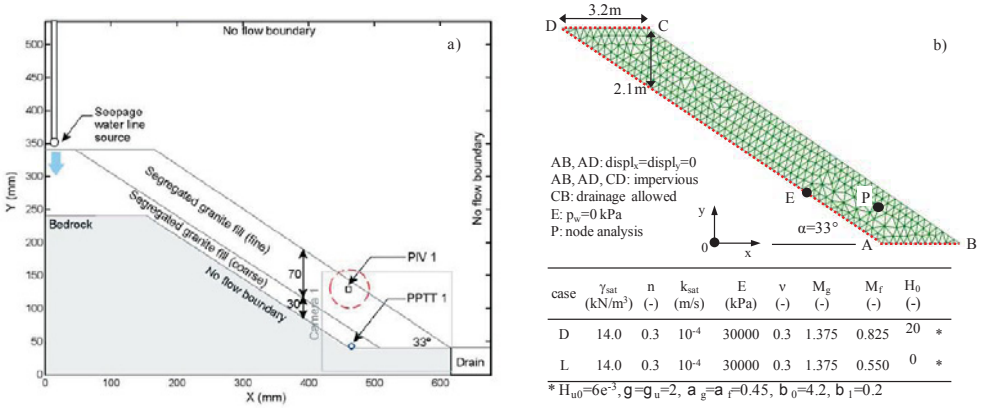

case	γ_{sat} (kN/m^3)	n (-)	k_{sat} (m/s)	E (kPa)	v (-)	M_g (-)	M_f (-)	H_0 (-)	
D	14.0	0.3	10^{-4}	30000	0.3	1.375	0.825	20	*
L	14.0	0.3	10^{-4}	30000	0.3	1.375	0.550	0	*

* $H_{u0}=6e^{-3}$, $g=g_u=2$, $a_g=a_f=0.45$, $b_0=4.2$, $b_1=0.2$

Fig. 6. (a) Centrifuge slope model [17] and (b) numerical slope model.

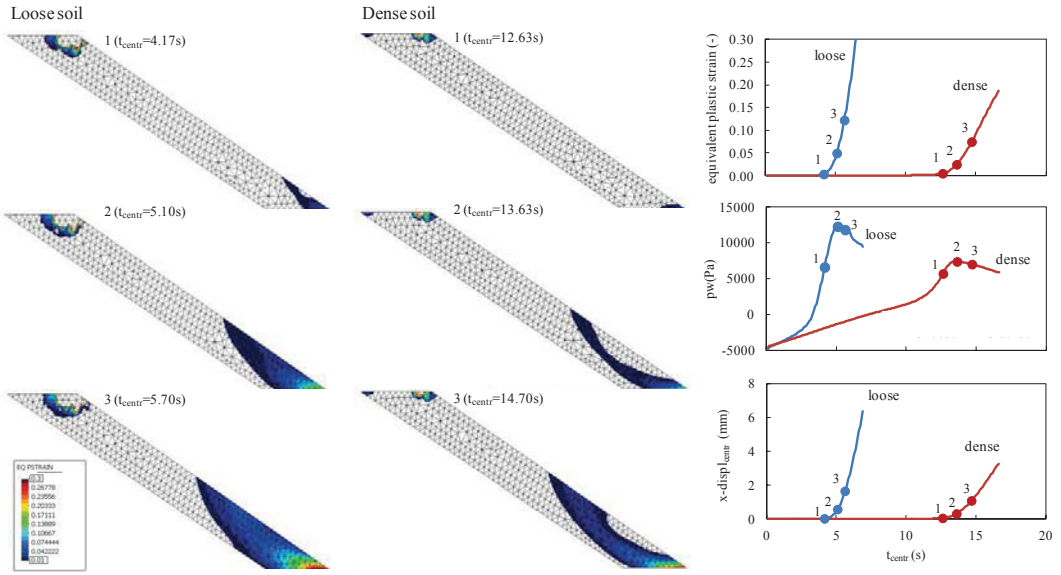

Fig. 7. Pore water pressures, equivalent plastic strains and x-displacements (at point P) for slopes of loose and dense soils.

3.3. Propagation stage

The propagation stage can be profitably addressed for well-documented real case histories as post-event information may include: depth of slip surface at source areas, landslide path, heights of propagating mass at specific points, erosion depths along the path, deposition heights and, in some cases, indirect data to be correlated to mass velocities such as super-elevation at bends[19] and characteristics of structures damage due to mass impact[37].

The case history of section 3.1 is analyzed; in particular, the paper refers to two major landslides triggered by the mechanism M1 at an altitude of 500 - 700 m a.s.l. with a total mobilized volume[18] of about 50,000 m^3; the triggered masses joined in a channel with steep flanks; then, the whole mass travelled about 1,500 meters of which 400 meters in the channel and 1,100 meters in a flatter piedmont area.

Numerical analyses refer to a 3×3m Digital Terrain Model (DTM) from which a topographic mesh of 105,534 nodes is derived. The initial masses are schematized through two set of 2,936 and 4,598 points initially 3 m spaced; initial soil heights are equal to 0.1 - 4 m inside the source areas[18]. A frictional model is assumed for the rheological behavior and rheological parameters are taken from literature[24]. It is worth mentioning that the landslide growth rate (sect 2.2) is assumed equal to 4×10^{-4} - 1×10^{-3} m^{-1}, that is within the range provided by literature[19,24].

Figure 8 shows that the bed entrainment greatly affects the landslide propagation stage. Whether only the channel is erodible (Fig. 8a), the simulated landslide travels much at the right-hand side; if the propagating mass can entrain material along the whole propagation path (Fig. 8b), the simulated bed entrainment causes material deposition and reduces the landslide run-out distance. In both cases SPH modeling provides: i) distinct propagation areas, ii) similar run-out distances, iii) run-out shorter than the observed one of about 400 m. Assuming an higher landslide growth rate along the whole propagation path, the field evidence is poorly reproduced as simulated landslide stops at the exit of the channel where a thick deposit is formed (Fig. 8c). Only whether calibrating rheology and entrainment parameters jointly, a satisfactorily back-analysis of the in-situ evidence is obtained for both the run-out distance and the extent of propagation-deposition zones (Fig. 8d). Simulated landslide lasts about time 60 seconds in agreement with literature[24] and eyewitnesses of inhabitants[13]. Minor mismatches arise at both the lateral sides of the propagation path; however, these discrepancies may be related to the simplified timing of failures (two masses fail at once) or topography peculiarities not well reproduced in the DTM. For case 8d (Fig. 8), the space-time evolution of pore water pressures (normalized to liquefaction pressure) is provided in figure 9 which shows the high variations of p_w simulated at the entry, inside and at the exit of the channel.

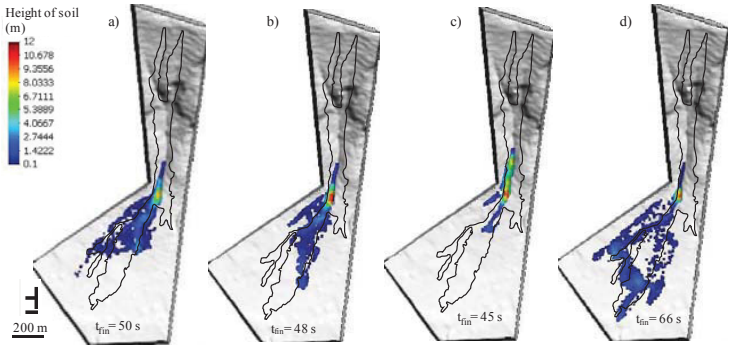

Fig. 8. Height of deposit simulated for different assumption on bed entrainment.

Uncertainties still affect the results achieved in the analyses. Novel physically-based entrainment laws should be introduced to capture better the onset of material entrainment and its development under time-dependent loading conditions related to the propagating of a liquefied mass over the ground surface. Particularly, solid concentration of propagating mass and the availability of solid particles along the landslide path are important factors which could be accounted for. Furthermore, an accurate bed entrainment analysis would require a proper rheological (or constitutive) model for the behavior of the interface between the propagating landslide and the ground surface.

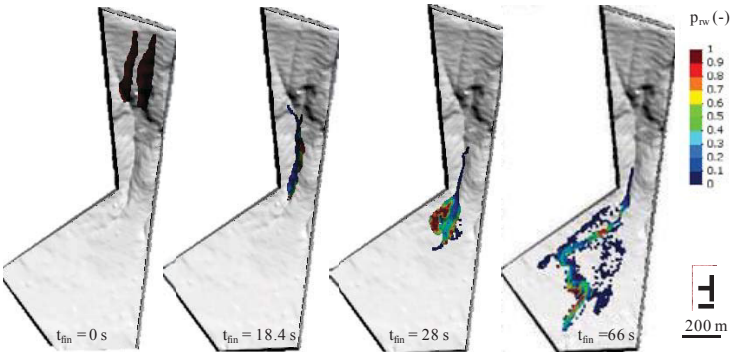

Fig. 9. Space-time evolution of pore water pressures (normalized to liquefaction pressure) at the entry, inside and at the exit of the channel.

On the other hand, fully 3D mathematical approaches capable to simulate more accurately the variations of pore water pressures inside the propagating mass could enhance the potential of numerical model towards a larger class of applications also including the dynamic impact of landslides against structures.

4. Concluding remarks

Numerical investigations jointed to experimental and field evidences point out important issues: i) pore water pressure is a primary factor in all the stages of landslides of the flow-type, ii) an advanced constitutive model is a necessary ingredient whether the post-failure stage is addressed, iii) a proper description of rheology and bed entrainment is fundamental to adequately assess the inundation areas.

Important challenges are still related to the gap between constitutive and rheological models to be filled through a global mathematical model for mechanical behavior of mixture of solid grains and pore fluid(s) under small/large deformations. Once this step will be done, a unified large-deformation based numerical tool might be implemented for fully simulating this type of landslides: from triggering to flow transition and until the mass stops.

Acknowledgments

Prof. Leonardo Cascini and Prof. Manuel Pastor deserve my special gratefulness since they constantly addressed me towards advanced analysis and modeling of flow-type landslides. Many thanks to Giuseppe Claudio Castorino, Luca Piciullo and Claudia Sacco for their valuable and enthusiastic contribution to this research.

I would like to dedicate this paper to the memory of the recently departed Prof. Giuseppe Sorbino. His vitality, optimistic nature, and many other human and scientific qualities will be very much missed.

References

1. Hungr O, Evans SG, Bovis MJ, Hutchinson, J.N. A review of the classification of landslides of the flow type. *Environmental and Engineering Geoscience 2001*;**8(3)**:221-238.
2. Hungr O, Leroueil S, Picarelli L. Varnes classification of landslide types, an update. Proc. of 11th Int. Symposium on Landslides: Landslides and Engineered Slopes, Banf, Canada June 3-8, 2012, Ed. E. Eberhardt, C. Froese, K. Turner, S. Leroueil, ISBN 978-0-415-62423-6; Balkema, Rotterdam, 2012, p. 47-58.
3. Cascini L, Cuomo S, Pastor M, Sorbino G, Piciullo L. Modeling of propagation and entrainment phenomena for landslides of the flow type: the May 1998 case study. Proc. of 11th Int. Symposium on Landslides: Landslides and Engineered Slopes, Banf, Canada June 3-8, 2012, Ed. E. Eberhardt, C. Froese, K. Turner, S. Leroueil, ISBN 978-0-415-62423-6, Balkema, Rotterdam, 2012,1723-1729.
4. Cascini L, Cuomo S, Pastor M, Sorbino G, Piciullo L. SPH run-out modelling of channelized landslides of the flow type. *Geomorphology 2014*, DOI: 10.1016/j.geomorph.2014.02.031. pp. 12.
5. Cascini L, Cuomo S, Pastor M, Sorbino G. Modelling of rainfall-induced shallow landslides of the flow-type. *ASCE's Journal of Geotechnical and Geoenvironmental Engineering 2010*; **1**:85-98.
6. Leroueil S. Natural slopes and cuts: movement and failure mechanisms. *Geotechnique 2001*: **51(3)**:197-243.

7. Darve F., Laouafa F. Instabilities in granular materials and application to landslides. *Mechanics of Cohesive frictional Materials 2000*;**58**:627-652.
8. Pastor M, Fernandez-Merodo JA, Gonzalez E, Mira P, Li T, Liu X. Modelling of landslides: (I). Failure mechanisms. In: Degradations and Instabilities in Geomaterials, CISM Course and Lectures No. 461, Darve F. and Vardoulakis I. (ed.), Springer-Verlag, 2004, 287-317.
9. Cascini L. The flowslides of May 1998 in the Campania region, Italy: the scientific emergency management. *Italian Geotechnical Journal 2004*;**2**:11-44.
10. Cascini L, Cuomo S, Guida D. Typical source areas of May 1998 flow-like mass movements in the Campania region, Southern Italy. *Engineering Geology 2008*;**96**:107-125.
11. Cascini L, Sorbino G, Cuomo S. Modelling of flowslides triggering in pyroclastic soils. Proc. Int. Conference on "Fast Slope Movements "Prediction and Prevention for Risk Mitigation", Napoli, Patron Ed. 1,2003,93-100.
12. Fiorillo F, Wilson RC. Rainfall induced debris flows in pyroclastic deposits, Campania (Southern Italy). *Engineering Geology 2004*;**75**:263-289.
13. Cascini L, Cuomo S, Sorbino G. Flow-like mass movements in pyroclastic soils: remarks on the modelling of triggering mechanisms. *Italian Geotechnical Journal 2005;***4**:11-31.
14. Cuomo S. Geomechanical modelling of triggering mechanisms for flow-like mass movements in pyroclastic soils. PhD dissertation at the University of Salerno, Italy, 2006, p. 274.
15. Baum RL, Godt JW, Coe JA. Assessing susceptibility and timing of shallow landslide and debris flow initiation in the Oregon Coast Range, USA. Proc. of International Conference on Debris-Flow Hazards Mitigation: Mechanics, Prediction, and Assessment, 2011, pp. 825-834.
16. Cascini L, Cuomo S, Pastor M, Sacco C. Modelling the post-failure stage of rainfall-induced landslides of the flow-type. *Canadian Geotechnical Journal 2013;***50(9)**:924-934.
17. Take WA, Bolton MD, Wong PCP, Yeung FJ. Evaluation of landslide triggering mechanisms in model fill slopes. *Landslides 2004*; **1**:173-184.
18. Cascini L, Guida D, Sorbino G. Il Presidio Territoriale. Una esperienza sul campo. Soveria Mannelli. Rubbettino. ISBN: 88-498-0962-X, 2005, pp. 139 (in Italian).
19. Revellino P, Hungr O, Guadagno FM, Evans SG. Velocity and runout prediction of destructive debris flows and debris avalanches in pyroclastic deposits, Campania region, Italy. *Environmental Geology 2004*;**45**:295-311.
20. Zienkiewicz OC, Chang CT, Bettess P. Drained, undrained, consolidating dynamic behaviour assumptions in soils. *Geotechnique 1980*;**30**: 385-395.
21. Zienkiewicz OC, Chan AHC, Pastor M, Shrefler BA, Shiomi T. *Computational Geomechanics 1999*. J.Wiley and Sons.
22. Pastor M, Li T, Liu X, Zienkiewicz OC. Stabilized low order finite elements for failure and localization problems in undrained soils and foundations. *Comput. Methods Appl. Mech. Engrg. 1999*;**174**:219-234.
23. Pastor M, Zienkiewicz OC, Chan AHC. Generalized plasticity and the modelling of soil behaviour. *Int. J. Numer. and Anal. Methods in Geomechanics 1990*;**14**: 151-190.
24. Pastor M, Haddad B, Sorbino G, Cuomo S, Drempetic V. A depth-integrated, coupled SPH model for flow-like landslides and related phenomena. *Int. J. Numer. Anal. Meth. Geomech 2009*, **33**:143-172.
25. Hutchinson JN. A sliding-consolidation model for flow slides. *Canadian Geotechnical Journal 1986*;**23**:115-126.
26. Pastor M, Quecedo M, Fernandez-Merodo JA, Herreros MI, Gonzalez E, Mira P. Modelling tailing dams and mine waste dumps failures. *Geotechnique 2002*;**528**:579-591.
27. Hungr O. A model for the runout analysis of rapid flow slides, debris flows, and avalanches. *Canadian Geotechnical J. 1995*;**32**:610-623.
28. Blanc T, Pastor M. A stabilized Smoothed Particle Hydrodynamics, Taylor-Galerkin algorithm for soil dynamics problems. *Int. J. Numer. Anal. Meth. Geomech. 2011*. DOI: 10.1002/nag.1082.
29. Pastor M, Crosta GB. Landslide runout: Review of analytical/empirical models for subaerial slides, submarine slides and snow avalanche. Numerical modelling. Software tools, material models, validation and benchmarking for selected case studies. Deliverable D1.7 for SafeLand Project http://www.safeland-fp7.eu/results/Documents/D1.7_revised.pdf., 2012.
30. Cuomo S, Pastor M, Vitale S, Cascini L. Improvement of irregular DTM for SPH modelling of flow-like landslides. Proc. of XII International Conference on Computational Plasticity. Fundamentals and Applications (COMPLAS XII), E. Oñate, D.R.J. Owen, D. Peric and B. Suárez (Eds). 3-5 September 2013, Barcelona, Spain. ISBN: 978-84-941531-5-0, 2013, pp. 1-10.
31. Geoslope. User's guide. GeoStudio 2004, Version 6.13. Geo-Slope Int. Ltd. Calgary, Canada, 2005.
32. Janbu N. Application of Composite Slip Surface for Stability Analysis. European Conference on Stability Analysis, Stockholm, Sweden, 1954.
33. Morgenstern NR, Price VE. The analysis of the stability of general slip surfaces. *Geotechnique 1965*;**151**:79-93.
34. Fredlund DG, Morgenstern NR, Widger RA. The shear strength of unsaturated soils. *Canadian Geotechnical Journal 1978*;**15**:313-321.
35. Lee YS, Cheuk CY, Bolton MD. Instability caused by a seepage impediment in layered fill slopes. *Canadian Geotechnical Journal 2008*; **45(10)**:1410-1425.
36. Prime N, Dufour F, Darve F. Modeling of landslides with a Finite Element Method with Lagrangian Integration Points. Computational Geomechanics, COMGEO II - Proceedings of the 2nd International Symposium on Computational Geomechanics 2011, 354-363.
37. Faella C, Nigro E. Dynamic impact of the debris flows on the constructions during the hydrogeological disaster in Campania-1998: failure mechanical models and evaluation of the impact velocity. Proc. Int. Conference on "Fast Slope Movements-Prediction and Prevention for Risk Mitigation". Patron Editore, Napoli, 2003, pp. 179-186.